

Elastic properties of B-C-N films grown by N₂-reactive sputtering from boron carbide targets

E. Salas,^{1,a)} R. J. Jiménez Riobóo,¹ J. Sánchez-Marcos,^{1,2} F. Jiménez-Villacorta,^{1,b)} A. Muñoz-Martín,³ J. E. Prieto,³ V. Joco,³ and C. Prieto^{1,c)}

¹*Instituto de Ciencia de Materiales de Madrid, Consejo Superior de Investigaciones Científicas, Cantoblanco, 28049 Madrid, Spain*

²*Dept. Química-Física Aplicada, Universidad Autónoma de Madrid, Cantoblanco, 28049 Madrid, Spain*

³*Centro de Microanálisis de Materiales, Universidad Autónoma de Madrid, Cantoblanco, 28049 Madrid, Spain*

(Received 23 October 2013; accepted 14 November 2013; published online 3 December 2013)

Boron-carbon-nitrogen films were grown by RF reactive sputtering from a B₄C target and N₂ as reactive gas. The films present phase segregation and are mechanically softer than boron carbide films (a factor of more than 2 in Young's modulus). This fact can turn out as an advantage in order to select buffer layers to better anchor boron carbide films on substrates eliminating thermally induced mechanical tensions. © 2013 AIP Publishing LLC. [<http://dx.doi.org/10.1063/1.4837655>]

I. INTRODUCTION

Boron-based compounds have been extensively investigated as hard coatings and as semiconductors for high-temperature applications.¹ They also present a wide diversity of functional properties ranging from wide band-gap insulators with very good thermoelectric properties at high temperatures^{2,3} to high-temperature superconductivity.⁴ The origin of these unique properties lies in their uncommon structure and bonding nature, which additionally may allow the growth of peculiar nanostructures when deposited on appropriate substrates.⁵ Boron carbide is especially interesting due to its exceptional mechanical properties⁶ that include high hardness (even at high temperatures), low friction coefficient, good wear capability, and high chemical stability. Theoretical studies show that BC₂N material has similar hardness properties as diamond and c-BN but with improved oxidation resistance.⁷ In the last few years, ternary systems based on B-C-N have been the subject of study, aimed to obtaining a combination of specific properties of boron carbide, cubic and hexagonal boron nitride oriented to the design and fabrication of materials⁸ with high thermal and chemical stability,⁹ low friction coefficient,¹⁰ high hardness,^{11–13} and good wear resistance.¹⁴

On the other hand, the large absorption cross section for thermal neutrons of the ¹⁰B isotope (that is 20% present in natural boron) allows a unique application of boron carbide in solid-state neutron detector for large-scale neutron source laboratories¹⁵ and even for general purpose neutron detection.¹⁶

Unfortunately, boron carbide and boron carbonitride thin films present delamination^{17,18} when the film thickness lies about 0.5 μm. The mismatch of mechanical properties

between the hard film and the substrate together with the existence of huge internal stresses are at the basis of the bad adhesion of the film to the substrate.^{19,20} This problem is, typically, overcome by the deposition of functionally graded multilayered (FGM) coatings to achieve a continuous transition between the substrate and the operating film.²¹

The mechanical behavior of the whole material is determined by the elastic properties of the components, where typically small amounts of elastic soft compound may worsen the hardness of the system. This fact becomes of special importance when carbon is one of the chemical components due to the possibility of the formation of graphite that may change drastically the mechanical properties of the whole material. The mechanical properties of thin films can be studied by measuring the surface acoustic wave velocity (*v*_{SAW}), which is directly related to the tensor of elastic constants of the film material. The study of the *v*_{SAW} dependence on film thickness and on the phonon propagation direction may deliver information about the compounds that actually determine the elastic properties of the coating.²² In this sense, Brillouin scattering is a non-destructive contactless technique that measures directly the thickness dependence of *v*_{SAW} as well as the substrate influence to obtain information about the elastic behavior of a coated substrate.

Several techniques such as RF magnetron sputtering,²³ pulsed laser deposition,²⁴ or chemical vapor deposition²⁵ have been used to deposit B-C-N compounds. One of the simplest processes is the preparation of ternary B-C-N films from B₄C targets by N₂-reactive sputtering,²⁶ in which the formation of hexagonal boron nitride was detected. Nevertheless, the composition of these B-C-N films is a matter of controversy since Freire *et al.*²⁶ and Linss *et al.*²⁷ concluded that B-C-N films present phase separation, while amorphous structure with atomic hybridation of B, C, and N atoms are reported by Zhou *et al.*²⁸ and Jia *et al.*²⁹

The aim of this work is twofold. First, to elucidate the existence of phase segregation in B-C-N films deposited on Si (100) substrates by reactive RF magnetron sputtering. For this purpose, infrared absorption and Raman spectroscopies

^{a)}Present address: SpLine Spanish CRG Beamline at the European Synchrotron Radiation Facilities, ESRF-BP 220-38043 Grenoble Cedex, France.

^{b)}Present address: Department of Chemical Engineering, Northeastern University, Boston, Massachusetts 02115, USA.

^{c)}Author to whom correspondence should be addressed. Electronic mail: cprieto@icmm.csic.es. Tel.: +34 913 349 000. Fax: +34 913 720 623.

as well as elastic recoil detection analysis by time of flight (ERDA-ToF) has been used to characterize the composition of the films. Second, High Resolution Brillouin Spectroscopy (HRBS) has been harnessed to measure v_{SAW} and obtain information about the mechanical properties of the obtained films. Additionally, in the case of phase segregation, the question arises whether the mechanical properties of the obtained films are adequate to allow the use of this kind of films as a FGM in order to solve the adhesion problems shown by boron carbide and boron carbonitride films.^{30,31}

II. EXPERIMENTAL

B-C-N thin films were deposited by RF magnetron reactive sputtering techniques at room temperature from a dense B_4C target and N_2 as reactive gas on Si (001) substrate. Starting from a residual pressure near 10^{-7} mbar in the preparation chamber, samples were deposited at 5×10^{-3} mbar, using different gas flow N_2/Ar ratios from 0% to 70%. The here presented study has been performed with films of thickness ranging from 20 to 100 nm deposited by using a RF power of 100 W to obtain typical deposition rates of 2 nm min^{-1} . The thickness of the films was precisely measured by low angle X-ray reflectivity on a Bruker D8 four-circle x-ray diffractometer.

The atomic composition of films was determined by means of ERDA-ToF spectroscopy performed at the Centro de Microanálisis de Materiales (CMAM) of the Universidad Autónoma de Madrid. This technique becomes especially useful when film components have smaller atomic masses than the substrate, as it is the case of boron carbide films. A 5-MV Cockcroft–Walton tandem accelerator was used to deliver a Br^{3+} ion beam with energy of 25 MeV. Measurements of ToF and energy were made in coincidence for each detected particle. Unambiguous identification of each detected particle is obtained by determining its mass. A thorough explanation of the experimental setup was provided elsewhere.²²

The chemical composition of the obtained films was characterized by using the Fourier Transform detection of infrared absorption spectroscopy (FTIR) (Varian 660 FTIR model spectrophotometer) and a homemade micro-Raman system, consisting on a Jobin-Yvon HR 460 monochromator, a cooled CCD detection system and Kaiser Super-Notch-Plus filters to suppress the elastic scattered light. The excitation light (514.5 nm line of an Ar^+ laser) was focused on the samples with an Olympus microscope and a $\times 100$ objective that collects also the scattered light.

HRBS has been used to study the elastic properties of the prepared samples by collecting information about surface acoustic waves.³² The backscattering geometry has been used to collect spectra without polarization analysis of the scattered light, since we are dealing with thin films on silicon substrates. A detailed description of the experimental set-up can be found elsewhere.^{33,34} A 2060-Beamlok Spectra Physics Ar-ion single mode laser is used as monochromatic light source ($\lambda = 514.5 \text{ nm}$) and a 3+3 Pass tandem Fabry-Perot interferometer from JRS Scientific Instruments is the analyser of the Brillouin spectrometer. The acoustic wave vector, k , is

determined by the momentum conservation between incident and scattered light by $k_{\text{scattered}}^{\text{light}} = k_{\text{incident}}^{\text{light}} \pm k$.

In backscattering geometry, k can couple with the acoustic surface waves via the ripple mechanism when the incoming light is polarized in the scattering (sagittal) plane. In this case, k is given by $k = 4\pi \sin \theta_s / \lambda$ (being θ_s the selected sagittal angle and λ the vacuum laser wavelength) and the corresponding sound velocity by $v_{\text{SAW}} = \omega / k$; with $\omega = 2\pi f$, where f represents the Brillouin frequency shift.

III. RESULTS AND DISCUSSION

Fig. 1(a) shows an example of ERDA-ToF data obtained for a B-C-N film deposited by N_2 -reactive sputtering, where every dot represents a detected event in the energy–time diagram. Each observed branch corresponds to atoms with different mass detected in the film. Since carbon, nitrogen, and oxygen have only one main isotope of 12, 14, and 16 u, respectively, and boron has the two isotopes of 10 and 11 u, branches may be easily identified by its corresponding nuclide present in the sample. Since the ToF coordinate is directly related to the film depth, integration of each branch showed in Fig. 1(b) gives a picture of the atomic content as a function of the film depth. For instance, a small amount of oxygen is detected at the film surface and at the film/substrate interface, which may straightforwardly be identified, respectively, with a sample post-deposition oxidation and with the native silicon oxide of the substrate. Additionally, after taking into account each cross section, the atomic

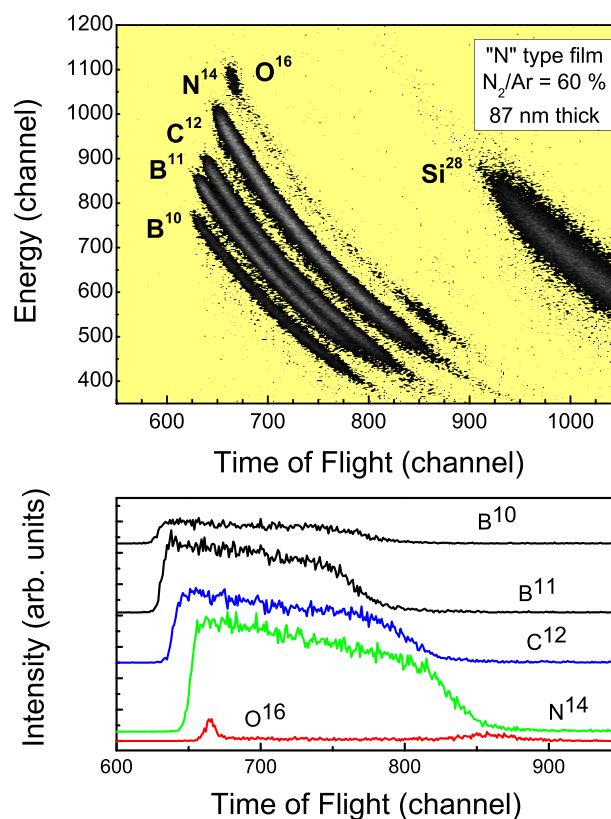


FIG. 1. (a) Energy vs. time of flight scatter plot of ERDA-ToF data obtained for a film of 87 nm thickness prepared by reactive sputtering with 60% of N_2 -content. (b) Intensity of branches corresponding to each of the elements found.

concentration of isotopes can be calculated by integration along the whole thickness of the sample.

Fig. 2 illustrates the evolution of the calculated concentration of the chemical elements present in the film as a function of the N_2 -content in the sputtering working gas. Error bars take into account dispersion between different samples of similar thickness prepared under similar conditions. It should be commented that the given oxygen content (near 5% for all samples) comprises the aforementioned amount of oxygen present at film interface and surface, being $<1\%$ across the film thickness.

By N_2 -reactive sputtering of a boron carbide target, nitrogen incorporates in the film in a nearly constant concentration of 40% when the working gas has a N_2 -content of 10% or higher. These results are in agreement with those reported by Freire *et al.*²⁶ The increase of the nitrogen content in the film is directly related with the decrease in boron content pointing towards a reactive sputtering of boron. On the other hand, no appreciable differences are observed between samples prepared with nitrogen in the 10% to 70% concentration range; thus considering the similarity between samples prepared with any N_2/Ar gas two types of film will be studied, labeled “N”-type for films deposited with any N_2/Ar mixture (independently of the N_2 -content in the sputtering gas), and “A”-type for Ar-sputtered.

Raman scattering and infrared-absorption (FTIR) vibrational spectroscopies were carried out in order to determine the composition of the “N”-type samples with the aim to be compared with those in the already studied “A”-type samples.²² Raman spectroscopy is an ideal non-destructive technique to check carbon structures³⁵ and FTIR spectroscopy is especially indicated to study boron-type vibrations in this BCN system, because their signals are not masked by the sp^2 -carbon modes, which are IR-forbidden.

Fig. 3(a) shows the experimental FTIR spectra of the films, revealing clear differences obtained for both types of samples. “A”-type samples show a wide contribution centered close to 1200 cm^{-1} and some typically crystalline narrow bands corresponding to the boron carbide icosahedral structure²⁶ at 1116 cm^{-1} (B_4C) and 1166 cm^{-1} (B_2C), to c-BN at

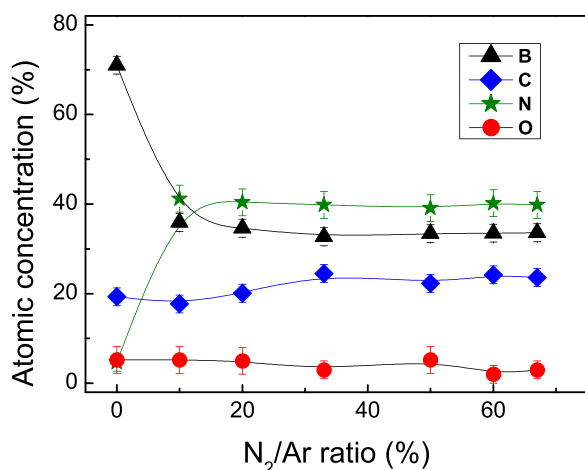


FIG. 2. Evolution of the concentration of the chemical elements present in the film as a function of the N_2 -content in the sputtering working gas.

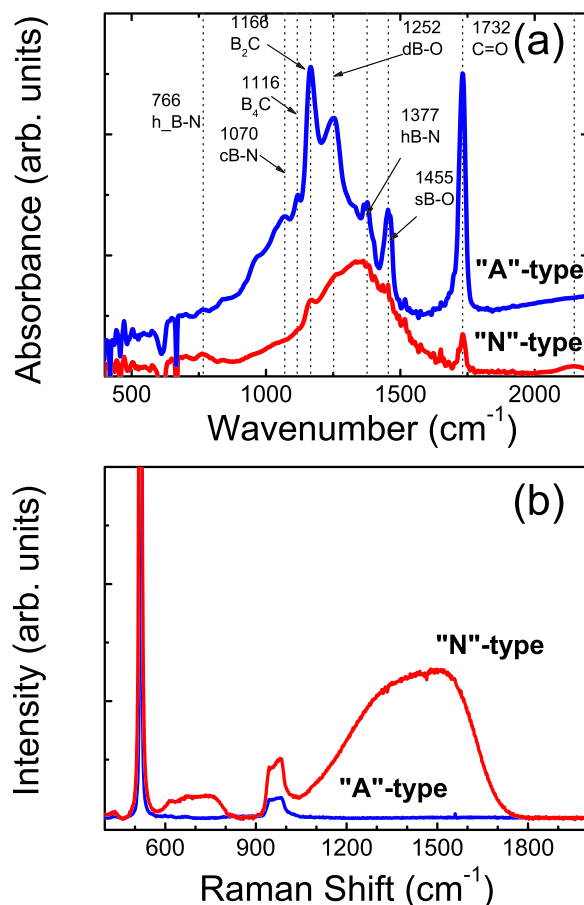


FIG. 3. (a) FTIR absorbance. (b) Raman scattering spectra of both types of films.

1070 cm^{-1} , to h-BN at 1377 cm^{-1} and to the B-O stretching mode at 1455 cm^{-1} . On the other hand, the “N”-type samples show a main non-crystalline band around 1360 cm^{-1} . This wide signal would be in agreement with an amorphous structure formed by disordered carbon structure (D-band at 1380 cm^{-1}),³⁵ and some small contributions of the same contribution detected in “A”-type samples. The characteristic peaks of boron oxide, around 1252 cm^{-1} and 1455 cm^{-1} , are also detected in both types of samples.

Raman spectra of “A” and “N” samples are shown in Fig. 3(b). Apart of the two signals from the Si substrate at 520 cm^{-1} and 970 cm^{-1} , “N”-type samples present two Raman contributions. A broad band from 1100 to 1700 cm^{-1} is associated with vibrations assigned to amorphous carbon that typically appear in carbon films (graphite G-band around 1537 cm^{-1} and disorder D-band, at 1380 cm^{-1}).^{26,36} Moreover, the contribution at the 600 – 800 cm^{-1} range is associated with B-B vibrations.³⁷ These results can be explained by the formation of segregated carbon structures from boron carbide in the nitrogen-reactive sputtering growth of B-C-N films.

The results obtained from vibrational spectroscopies suggest the existence of phase segregation in “N”-type samples, mainly consisting of amorphous carbon and hexagonal boron-nitride with a non negligible amount of B_4C . In addition a boron oxide layer, present at the top surface of “N”-type samples, was unveiled by ERDA-ToF measurements.

Since the B-C-N films are not transparent, in the study of their elastic properties by HRBS only information about surface acoustic wave velocity (v_{SAW}) can be collected. For the type of film/substrate combination we are considering, v_{SAW} behaves as a monotonous function of the product of sound wave vector and film thickness (kh). This function has as limiting values the surface acoustic wave velocity value corresponding to the substrate (for h approaching to zero) and the velocity value of the surface acoustic wave in a bulk of the same nature as the film (for big enough h). A nonlinear combination of the elastic constants of substrate and film materials determines the v_{SAW} values. For very thin films ($kh < 0.5$, or typically $h < 30$ nm), v_{SAW} approaches the substrate value and for thick enough films ($kh > 10$, or typically $h > 550$ nm) v_{SAW} shows the corresponding elastic bulk values of the film material.^{38,39}

Surface acoustic wave velocities in “N”-type samples were obtained by means of HRBS at kh values of 0.65 and 1.69. In this way, it is easier to establish comparisons with velocities previously measured in “A”-type samples.²² These kh values were selected in a narrow range delimited by the sufficient SAW velocity variation respect to the substrate and by keeping good optical quality. The kh values were tuned by the appropriate incident angle θ_s in order to improve the signal to noise ratio and regarding the films thickness of 29 nm and 80 nm, respectively.

Fig. 4 shows the experimental data of v_{SAW} measurements of surface acoustic waves travelling along the [110] direction (defined by the silicon wafer) for two “N”-type samples (28.5 nm and 80.3 nm thick) as a function of the kh co-ordinate. An estimation of those obtained values has considered the h-BN, the $\text{B}_{5.6}\text{C}$, the graphitic amorphous carbon (a-C) and the B_2O_3 compounds revealed by FTIR and Raman spectroscopies. For this purpose, the SAW velocity dependence for these polycrystalline films on Si(001) along the [110] direction has been simulated (shown in Fig. 4). It should be noted that the experimentally obtained SAW velocity for “N”-type samples increases with kh values as for

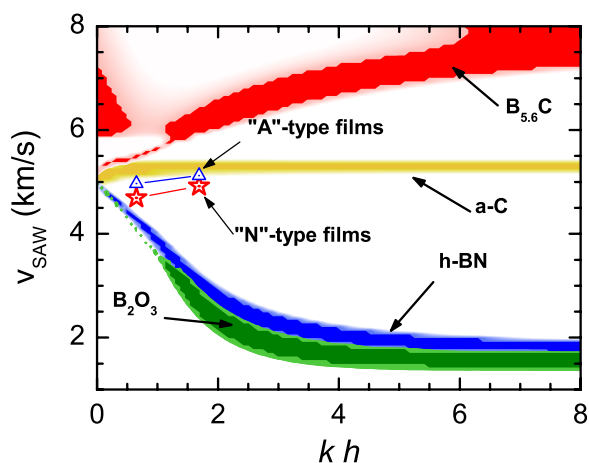


FIG. 4. Experimental v_{SAW} values of the “N”-type (circles), “A”-type samples (down triangles), and contour plot of the numerical simulation of the SAW velocity dependence of several polycrystalline films (B_2O_3 , h-BN, graphitic amorphous carbon, and $\text{B}_{5.6}\text{C}$) on Si (001) along the [110] direction.

the polycrystalline graphite and the boron carbide and conversely to the decrease obtained for h-BN films on silicon.

Fig. 5 shows the simulation of the azimuthal dependence of surface acoustic waves at the Si (001) substrate and the obtained velocities for the “A”- and “N”-samples evaluated at $kh = 0.65$ and $kh = 1.69$. However, HRBS is sensitive to the surface symmetry by performing an azimuthal scan to measure the dependence of surface phonons travelling along different directions contained in the surface plane, even for polycrystalline films.^{34,36} It may be noted that pure surface phonons are only travelling along $[\pm 1 \ 0 \ 0]$ and $[0 \pm 1 \ 0]$ directions and pseudo-surface phonons are easily detected near $[\pm 1 \pm 1 \ 0]$ directions; for intermediate angles, both surface and pseudo-surface phonons are present but with very small intensity in HRBS experiments making detection extremely difficult in the patterned region of the figure.

As expected in a (001) plane of the cubic symmetry imposed by the silicon substrate, the maximum and minimum v_{SAW} values are found for phonons traveling along the [110] and [100] crystallographic directions, respectively. It should be highlighted that SAW velocity in “N”-type samples is always smaller than velocity measured in “A”-type (about 4%) and lower than the Si (100) values.

Although “N”- and “A”-type of samples present clear similarities in their elastic behavior, there are relevant differences that need explanation. The fact that v_{SAW} of the “N”-samples is always lower than the v_{SAW} of the Si (100) substrate implies that we are dealing with a “slow on fast system” and an increase of kh values should imply a decrease in v_{SAW} of the system.⁴⁰ This is unlike to the experimental findings showing an increase of v_{SAW} as kh increases, but analogue to that found in “A”-samples, explained by the existence of a B_2O_3 layer on the top of the “A” type thin films.²² Moreover, regarding the atomic and chemical composition differences between the “N”- and “A”-type films, it becomes clear that in the case of the “N”-type films, BCN ternary compounds are not present to explain the elastic behavior and, contrary to the “A”-type films, BC compounds

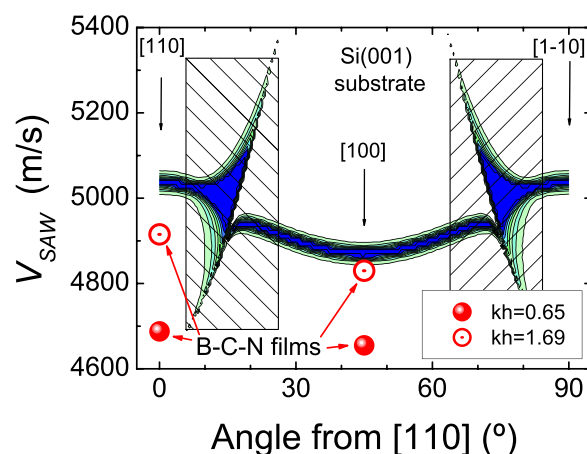


FIG. 5. Contour plot of the numerical simulation of the azimuthal dependence of the surface acoustic waves velocity (v_{SAW}) in Si (001). Experimental values obtained for the “N”-type samples (full and open circles corresponding to $kh = 0.65$ and $kh = 1.69$, respectively). The angular regions marked in patterned rectangle represent pseudo surface acoustic waves regions.

are present only in a small amount. Thus, the “N”-type films are mainly formed by graphitic amorphous carbon and smaller amounts of h-BN and boron carbide. This difference in composition can explain the lower v_{SAW} values of the “N”-type films compared to the “A”-type ones.

In order to quantify these differences, numerical simulations of the azimuthal and sagittal (kh) dependences of v_{SAW} have been performed. The calculation code, developed by Every and coworkers,⁴¹ uses the Green’s function formalism to simulate the intensity of scattered light due to the interaction of the incident light with the rippled surface. In this way, it is possible to calculate the behaviour of SAW velocity in an opaque material formed by one or more layers on a substrate as a function of the azimuthal angle and the kh product. For this purpose, inputs are density and elastic constants of layer and substrate.

In the present case, the model system is formed by a Si (001) substrate covered by a B-C-N film and a B_2O_3 layer on top. The composition of the B-C-N film must be compatible with the experimental values obtained by ERDA-ToF, FTIR and Raman spectroscopy. Thus, the B-C-N film must contain h-BN, BC and a-C, being the latter the most important component in terms of weight percentage. It is also important to remind that during reactive sputtering a big amount of N_2 is typically occluded in the film not being part of any nitride compound.

Since the sputtering technique promotes amorphous or, at least, polycrystalline microstructure in the deposited films, the elastic constants to be used in the simulations must be performed accordingly. Therefore, the Voigt-Reuss-Hill (VRH) average⁴² elastic constants for each compound were calculated from the density and elastic constants reported for $\text{B}_{5,6}\text{C}$,⁴³ h-BN,⁴⁴ boron oxide⁴⁵ and amorphous carbon³⁶ sputtered films. Table I summarizes the densities and the VRH averaged elastic constants in addition to the HRBS-measured elastic constants of the Si substrate.⁴⁶

Fig. 6 shows the comparison between measured SAW velocity and simulation. In order to fit experimental data, we have assumed that the “N”-type films are formed by a B-C-N layer covered on top with a B_2O_3 layer. The best results were obtained by using a B-C-N layer consisting of 59 at. % of a-C, 21 at. % of $\text{B}_{5,6}\text{C}$ and 20 at. % of h-BN. This composition is in agreement with the element ratio obtained by ERDA-ToF, with the exception of nitrogen for which some amount is expected to be occluded in its molecular form. The agreement

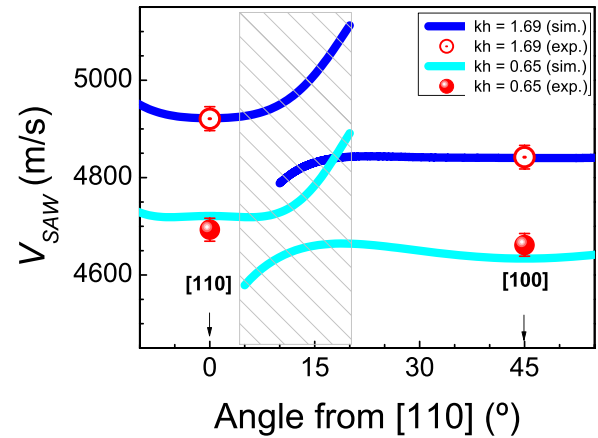


FIG. 6. Comparison between numerical simulations (lines) and experimental data (full circles) of the azimuthal dependence of the v_{SAW} .

between experimental data and simulation is excellent in the case of the 80.3 nm thick “N”-film ($kh = 1.69$) for both crystalline substrate directions, with a B_2O_3 overlayer of 10.6 nm. The 28.5 nm thick “N”-film ($kh = 0.65$) shows also good agreement for both directions, being the difference between experiment and simulation of the order of 0.5%. In this later case, simulation yields a B_2O_3 overlayer of 15.7 nm.

Comparison of “N” and “A” type samples²² leads to conclude that in B-C-N films (“N” type samples) the obtained mixture of amorphous carbon, boron carbide and boron nitride is responsible for the observed decrease of v_{SAW} values (about 4%) respect to that in B-C films (“A” type samples), which are mainly comprised by boron carbide.

A very interesting point is the fact that the longitudinal elastic constants, c_{11} , and especially the shear elastic constants, c_{44} , describing the “N” and “A” type films are very different conveying very different values of the corresponding Young’s moduli (E) for B-C-N films $E = 165.62$ GPa and for B-C films $E = 460.05$ GPa.

This fact can be used in an advantageously way when looking for buffer layers in order to improve the anchoring of boron carbide or boron carbo-nitride films used as coatings on metallic substrates. This is especially important in the case of temperature-induced tensions, where the difference in linear expansion coefficients between substrate and deposited film plays an important role. Taking into account the empirical behavior in which lower Young’s modulus correlate with higher linear thermal expansion coefficient,⁴⁷ B-C-N layers are suitable to constitute a functional graded material to solve the problem of delamination in the coating of polycrystalline aluminum ($E = 67.733$ GPa)⁴⁸ with ^{10}B -enriched boron carbide films to be used in neutron detection.^{15,49} The fact that the obtained elastic modulus for B-C-N films is in between that of boron carbide and aluminum lead to propose them as intermediate layers for the anchoring of B_4C on aluminum in the design of new neutron detectors.

IV. CONCLUSIONS

B-C-N thin films were deposited by reactive RF magnetron sputtering from a B_4C target on Si (001) substrates using N_2 as reactive gas. The structural and compositional

TABLE I. Density and VRH-averaged elastic constants of the compounds used for the numerical simulations of the dependence of the v_{SAW} . The last column gives the reference where values were reported. B-C-N* row corresponds to the obtained values for the “N”-type films in the present work.

	ρ (g/cm ³)	c_{11} (GPa)	c_{44} (GPa)	c_{12} (GPa)	E (GPa)	Ref.
Si	2.329	162	76	62		46
Al	2.702	111	25	61	67.7	48
B_2O_3	1.820	20.5	5.8	8.9	15.11	45
h-BN	2.180	39.0	14.34	10.32	34.7	44
a-C	2.16	540.6	62.2	416.2	178.5	36
$\text{B}_{5,6}\text{C}$	2.52	497.6	195.6	106.5	460	43
B-C-N (*)	2.1604	283.7	60.72	162.2	165.6	

characterization carried out by ERDA-ToF, Raman and FTIR shows that nitrogen incorporation into boron carbide is not effective and results in phase segregation, yielding the formation of amorphous carbon and hexagonal structured boron nitride compounds. The formation of a boron oxide layer on the sample surface is also reported as already observed in previously studied boron carbide samples. Elastic properties in nitrided boron carbide thin films were studied by means of high resolution Brillouin spectroscopy. The combination of experimental data with numerical simulations renders a film composition that agrees with the picture obtained from atomic and chemical characterization techniques. As a result, the elastic behavior of these samples is driven by amorphous carbon compound and is influenced by hexagonal boron nitride and surface boron oxide. This fact explains that SAW velocities measured in nitrided boron carbide thin films are lower than in previously studied boron carbide thin films. The corresponding Young's modulus is much lower than that of B_{5.6}C but clearly larger than typical values for polycrystalline metals. Thus, B-C-N films could be advantageously used as buffer layers between hard coating layers and metallic substrates in order to provide mechanical stability under temperature oscillations.

ACKNOWLEDGMENTS

This work has been supported by Spanish MINECO under contracts MAT2009-08786 and MAT2012-37276-C03-01 as well as by the Madrid Regional Government though contract S2009/MAT-1756. Special thanks are given to Professor A. G. Every for the v_{SAW} simulation code.

- ¹C. Wood and D. Emin, *Phys. Rev. B* **29**, 4582 (1984).
- ²Y. Kumashiro, T. Yokoyama, A. Sato, and Y. Ando, *J. Solid State Chem.* **133**, 314 (1997).
- ³K. Kamimura, T. Yoshimura, T. Nagaoka, M. Nakao, Y. Onuma, and M. Makimura, *J. Solid State Chem.* **154**, 153 (2000).
- ⁴J. Nagamatsu, N. Nakagawa, T. Muronaka, Y. Zentani, and J. Akimitsu, *Nature* **410**, 63 (2001).
- ⁵L. M. Cao, H. Tian, Z. Zhang, X. Y. Zhang, C. X. Gao, and W. K. Wang, *Nanotechnology* **15**, 139 (2004).
- ⁶L. G. Jacobsohn and M. Nastasi, *Surf. Coat. Technol.* **200**, 1472 (2005).
- ⁷J. L. He, L. C. Guo, E. Wu, X. G. Luo, and Y. J. Tian, *J. Phys.: Condens. Matter* **16**, 8131 (2004).
- ⁸T. H. Tsai, T. S. Yang, C. L. Cheng, and M. S. Wong, *Mater. Chem. Phys.* **72**, 264 (2001).
- ⁹D. C. Reigada and F. L. Freire, *Surf. Coat. Technol.* **142–144**, 889 (2001).
- ¹⁰E. Martinez, A. Lousa, and J. Esteve, *Diamond Relat. Mater.* **10**, 1892 (2001).
- ¹¹C. Morant, P. Prieto, J. Bareno, J. M. Sanz, and E. Elizalde, *Thin Solid Films* **515**, 207 (2006).
- ¹²S. Ulrich, T. Theel, J. Schwan, and H. Ehrhardt, *Surf. Coat. Technol.* **97**, 45 (1997).
- ¹³V. Linss, I. Hermann, N. Schwarzer, U. Kreissig, and F. Richter, *Surf. Coat. Technol.* **163–164**, 220 (2003).
- ¹⁴Y. Chen, Y. W. Chung, and S. Y. Li, *Surf. Coat. Technol.* **200**, 4072 (2006).
- ¹⁵C. Hoglund, J. Birch, K. Andersen, T. Bigault, J. C. Buffet, J. Correa, P. van Esch, B. Guerard, R. Hall-Wilton, J. Jensen, A. Khaplanov, F. Piscitelli, C. Vettier, W. Vollenberg, and L. Hultman, *J. Appl. Phys.* **111**, 104908 (2012).
- ¹⁶A. N. Caruso, *J. Phys.: Condens. Matter* **22**, 443201 (2010).
- ¹⁷M. U. Guruz, V. P. Dravid, and Y. W. Chung, *Thin Solid Films* **414**, 129 (2002).
- ¹⁸K. Sell, S. Ulrich, E. Nold, J. Ye, H. Leiste, M. Stuber, and H. Holleck, *Surf. Coat. Technol.* **174–175**, 1121 (2003).
- ¹⁹M.-L. Wu, J. D. Kiely, T. Klemmer, Y.-T. Hsia, and K. Howard, *Thin Solid Films* **449**, 120 (2004).
- ²⁰S. Ulrich, H. Ehrhardt, J. Schwan, R. Samlenski, and R. Brenn, *Diamond Relat. Mater.* **7**, 835 (1998).
- ²¹T. Tavsanoğlu, M. Jeandin, O. Addemir, and O. Yucel, *Solid State Sci.* **14**, 1717 (2012).
- ²²E. Salas, F. Jiménez-Villacorta, J. Sánchez-Marcos, R. J. Jiménez-Riobóo, A. Muñoz-Martín, J. E. Prieto, V. Joco, and C. Prieto, *Phys. Status Solidi A* **210**, 513 (2013).
- ²³D. H. Kim, E. Byon, S. Lee, J.-K. Kim, and H. Ruh, *Thin Solid Films* **447**, 192 (2004).
- ²⁴A. Perrone, A. P. Caricato, A. Luches, M. Dinescu, C. Ghica, V. Sandu, and A. Andrei, *Appl. Surf. Sci.* **133**, 239 (1998).
- ²⁵M. C. Polo, E. Martínez, J. Esteve, and J. L. Andujar, *Diamond Relat. Mater.* **8**, 423 (1999).
- ²⁶F. L. Freire, D. C. Reigada, and R. Prioli, *Phys. Status Solidi A* **187**, 1 (2001).
- ²⁷V. Linss, S. E. Rodil, P. Reinke, M. G. Garnier, P. Oelhafen, U. Kreissig, and F. Rischter, *Thin Solid Films* **467**, 76 (2004).
- ²⁸Z. F. Zhou, I. Bello, M. K. Lei, K. Y. Li, and C. S. Lee, *Surf. Coat. Technol.* **128**, 334 (2000).
- ²⁹F. Jia, C. Zhuang, C. Guan, J. Zhao, Y. Bai, and X. Jiang, *Vacuum* **85**, 887 (2011).
- ³⁰I. Caretti, J. M. Albella, and I. Jimenez, *Diamond Relat. Mater.* **16**, 1445 (2007).
- ³¹T. Tavsanoğlu, O. Yucel, O. Addemir, and M. Jeandi, in *Supplemental Proceedings: TMS2008—Materials Processing and Properties* (2008), Vol. 1, p. 279.
- ³²J. R. Sandercock, *Light Scattering in Solids III*, Applied Physics Vol. 51, edited by M. Cardona and G. Güntherodt (Springer-Verlag, Berlin, 1989).
- ³³R. J. Jiménez-Riobóo, M. García-Hernández, C. Prieto, J. J. Fuentes-Gallego, E. Blanco, and R. Ramírez del Solar, *J. Appl. Phys.* **81**, 7739 (1997).
- ³⁴E. Salas, R. J. Jiménez-Riobóo, C. Prieto, and A. G. Every, *J. Appl. Phys.* **110**, 023503 (2011).
- ³⁵J. Filik, *Spectroscopy Europe* **17**, 10 (2005).
- ³⁶E. Salas, R. J. J. Riobóo, A. de Andrés, and C. Prieto, *Eur. Phys. J. B* **75**, 151 (2010).
- ³⁷V. Kulikovskiy, V. Vorlicek, P. Bohac, R. Ctvrtlik, M. Stranyanek, A. Dejnek, and L. Jastrabik, *Diamond Relat. Mater.* **18**, 27 (2009).
- ³⁸G. A. D. Briggs, *Advances in Acoustic Microscopy* (Plenum Press, New York, 1995), Vol. 1.
- ³⁹R. J. J. Riobóo, E. Rodríguez-Cañas, M. Vila, C. Prieto, F. Calle, T. Palacios, M. A. Sánchez, F. Omnès, B. Assouar, and O. Elmazria, *J. Appl. Phys.* **92**, 6868 (2002).
- ⁴⁰C. Sumanya, J. D. Comins, and A. G. Every, *J. Phys.: Conf. Ser.* **92**, 012103 (2007).
- ⁴¹X. Zhang, J. D. Comins, A. G. Every, P. R. Stoddart, W. Pang, and T. E. Derry, *Phys. Rev. B* **58**, 13677 (1998).
- ⁴²G. Grimvall, in *Thermophysical Properties of Materials*, edited by E. P. Wohlfarth (North-Holland, Amsterdam, 1986).
- ⁴³K. J. McClellan, F. Chu, J. M. Roper, and I. Shindo, *J. Mater. Sci.* **36**, 3403 (2001).
- ⁴⁴V. M. Mathew, C. S. Menon, and K. P. Jayachandran, *J. Mater. Sci.* **37**, 5237 (2002).
- ⁴⁵M. A. Ramos, J. A. Moreno, S. Vieira, C. Prieto, and J. F. Fernández, *J. Non-Cryst. Solids* **221**, 170 (1997).
- ⁴⁶A. de Bernabé, C. Prieto, D. Cáceres, I. Vergara, A. G. Every, and H. E. Fischer, *Phys. Status Solidi A* **188**, 1023 (2001).
- ⁴⁷R. J. Arenz, in *Proceedings of the 2005 SEM Annual Conference and Exposition on Experimental and Applied Mechanics—Experimental Mechanics Applied to Advanced Materials Systems*, SEM, Orlando, 2005.
- ⁴⁸B. A. Auld, *Acoustic Fields and Waves in Solids* (Krieger Publishing Comp., Florida, 1990), Vol. 1.
- ⁴⁹J. Birch, J. C. Buffet, J. Correa, P. van Esch, B. Guérard, R. Hall-Wilton, C. Höglund, L. Hultman, A. Khaplanov, and F. Piscitelli, *IEEE Trans. Nucl. Sci.* **60**, 871 (2013).